

# Exciton–vibrational interaction of the Fröhlich type in quasi-zero-size systems

A. V. Fedorov and A. V. Baranov

*S. I. Vavilov State Optical Institute, 199034 St. Petersburg, Russia*

(Submitted 28 March 1996)

*Zh. Éksp. Teor. Fiz.* **110**, 1105–1120 (September 1996)

We derive analytic expressions for the matrix elements of the exciton–vibrational interaction of the Fröhlich type in spherical semiconducting crystals. The selection rules that allow for transitions involving *LO*-phonons between arbitrary excitonic states are established. We show that because of a three-dimensional spatial limitation, the exciton–phonon scattering in transitions between states with the same parity loses its forbidden nature. The size dependence of the interaction matrix elements is studied. We demonstrate that nanocrystals constitute a Jahn–Teller system and for certain sizes exhibit a vibrational resonance. We estimate the Huang–Rees factor and find that it strongly depends on the size of the nanocrystal. On the basis of these results we calculate the form functions of multiphonon light absorption. The proposed method of calculating the exciton energy spectrum makes it possible to take into account the effect of a three-dimensional spatial constraint on electron–hole relative motion.

© 1996 American Institute of Physics. [S1063-7761(96)02509-7]

## 1. INTRODUCTION

In recent years, extensive experimental and theoretical research has been done in the field of quasi-zero-size structures. The reason for this is that as the linear dimensions of a semiconducting crystal diminish to a size of the order of the Bohr exciton radius  $R_{ex}$ , there emerges an exceptionally interesting object which, partially retaining the properties of the initial material, acquires features characteristic of molecules or impurity centers. The best studied manifestation of the three-dimensional spatial constraint (three-dimensional confinement) of semiconducting structures is the size quantization of the energy spectrum of quasiparticle: electrons and holes, excitons, phonons, etc.<sup>1–3</sup> Another important manifestation of three-dimensional confinement is the modification of the interaction of the quasiparticles with each other<sup>4</sup> and with external fields (see, e.g., Ref. 5).

Depending on the ratio of the characteristic size  $R$  of the semiconducting nanostructure and the Bohr exciton radius, three cases are usually identifiable: the weak confinement, or excitonic, regime ( $R > R_{ex}$ ), the intermediate confinement regime ( $R \sim R_{ex}$ ), and the strong confinement regime ( $R < R_{ex}$ ). This paper deals with the first, for which it is still meaningful to speak of an exciton as a composite quasiparticle consisting of an electron and hole coupled by the Coulomb interaction. At the same time, in contrast to bulk material, the motion of an exciton in a quasi-zero-size structure is not translationally invariant, i.e., the wave-vector conservation law is not true here. More than that, because of three-dimensional confinement, the very concept of an exciton wave vector loses all meaning, and excitonic bands characteristic of the bulk material split into discrete size-quantization levels. The lack of translational symmetry and the fact that there is size quantization lead to a considerable modification of the exciton–phonon interaction. In particular, in the best-studied nanostructures based on semiconductors with relatively high ionicity ( $A_1B_7$ ,  $A_2B_6$ , and  $A_3B_5$ ) the exciton–vibrational interaction of the Fröhlich type

changes considerably. As a result the polar scattering of excitons by *LO*-phonons in transitions between excitonic states of the same parity (including intralevel transitions) loses its forbidden nature. Here the parity is related to the relative motion of the electron and hole.

The fact that the diagonal (adiabatic) part of the exciton–phonon interaction is nonzero and that the energy spectrum is discrete makes the nanostructure similar in some respects to a molecule or impurity center and allows a description of its optical properties that uses, after appropriate modifications, the models and methods developed by the theory of multiphonon transitions in local systems.<sup>6–8</sup>

There have been many papers devoted to the polar interaction of the electron subsystem of quasi-zero-size structures with *LO*-phonons (see, e.g., Refs. 9–11), with the predominant role of this interaction in resonant Raman and hyper-Raman scattering of light repeatedly confirmed in experiments.<sup>12,13</sup> Obviously, no less important is its role in absorption and luminescence. However, the exciton–phonon interaction of the Fröhlich type in the weak confinement regime has not been thoroughly studied and requires further investigation.

A fact of special interest is that quasi-zero-size systems exhibit, as will be shown below, a Jahn–Teller effect induced by *LO*-phonons. Under certain conditions there is vibrational resonance between the excitonic states, which makes possible the formation of tightly bound exciton–phonon complexes.<sup>14,15</sup>

## 2. POLAR INTERACTION OF EXCITONS WITH *LO*-PHONONS IN QUANTUM DOTS

We restrict our discussion to the polar scattering of excitons by *LO*-phonons in quantum dots (i.e., spherical nanocrystals), which serve as an object of investigation in most experiments.<sup>16</sup> We assume that the potential of a quantum dot has infinitely high walls. In many cases this approximation is justified for semiconducting nanocrystals embed-

ded in an insulator matrix. We also ignore surface optical modes and the relationship between  $LO$ -phonons and  $TO$ -phonons.<sup>10</sup> Then the potential  $\Phi(\mathbf{r})$  of the macroscopic field generated by  $LO$ -phonons in a spherical nanocrystal can be written as follows<sup>9</sup>:

$$\Phi(\mathbf{r}) = \sum_{nlm} f_{nl} \left( j_l \left( \xi_{nl} \frac{r}{R} \right) Y_{lm}(\theta, \varphi) a_{nlm} + j_l \left( \xi_{nl} \frac{r}{R} \right) Y_{lm}^*(\theta, \varphi) a_{nlm}^+ \right), \quad (1)$$

where  $R$  is the quantum-dot radius,  $j_l(x)$  and  $Y_{lm}(\theta, \varphi)$  are the spherical Bessel function and spherical harmonics,  $\xi_{nl}$  is the  $n$ th root of the equation  $j_l(\xi_{nl}) = 0$ ,  $a_{nlm}^+$  and  $a_{nlm}$  are the creation and annihilation operators of an  $LO$ -phonon of the  $\{nlm\}$  mode with frequency  $\omega_{nl}^{LO}$ ,  $l$  and  $m$  are the angular momentum and its projection, and the normalization factor  $f_{nl}$  is given by

$$f_{nl} = \frac{1}{\xi_{nl} j_{l+1}(\xi_{nl})} \left[ \frac{4\pi\hbar\omega_{nl}^{LO}}{R} \left( \frac{1}{\varepsilon_\infty} - \frac{1}{\varepsilon_0} \right) \right]^{1/2}, \quad (2)$$

with  $\varepsilon_\infty$  and  $\varepsilon_0$  the high- and low-frequency dielectric constants of the bulk material. According to Refs. 17 and 18, the exciton potential energy is

$$V = -e(\Phi(\mathbf{r}_e) - \Phi(\mathbf{r}_h)), \quad (3)$$

where  $\mathbf{r}_e$  and  $\mathbf{r}_h$  are the radius vectors of the electron and hole, and hence the exciton-phonon interaction operator has the form

$$H_{ex-LO} = \sum_{\nu_1 \nu_2} \sum_{nlm} \left( V_{nlm} \begin{pmatrix} \nu_2 \\ \nu_1 \end{pmatrix} a_{nlm} + V_{nlm}^* \begin{pmatrix} \nu_1 \\ \nu_2 \end{pmatrix} a_{nlm}^+ \right) b_{\nu_2}^+ b_{\nu_1}. \quad (4)$$

Here  $b_\nu^+$  and  $b_\nu$  are the exciton creation and annihilation operators in state  $\nu$ , and the label  $\nu_i$  with  $i = 1, 2$  stands for the set of quantum number of an excitonic state,  $\{n'_i, l'_i, m'_i; n_i, l_i, m_i\}$ , where the primed quantities characterize the motion of the exciton as a whole, and the unprimed, the relative motion of the electron and hole.

We assume that the exciton wave function is the product of the wave functions of relative and translational motions:

$$\Psi_{\nu_i}(\mathbf{r}_e, \mathbf{r}_h) = \psi_{n_i, l_i, m_i}(\mathbf{x}) \Psi_{n'_i, l'_i, m'_i}(\mathbf{X}), \quad (5)$$

$$\mathbf{x} = \mathbf{r}_e - \mathbf{r}_h, \quad \mathbf{X} = \rho_e \mathbf{r}_e + \rho_h \mathbf{r}_h, \quad (6)$$

$$\rho_e = \frac{m_h}{M}, \quad \rho_h = \frac{m_e}{M}, \quad M = m_e + m_h, \quad (7)$$

each of which in turn separates into radial and angular parts, with the latter being simply a spherical harmonic, in view of the symmetry of the problem. In (7) the quantities  $m_e$  and  $m_h$  are the effective electron and hole masses.

Under fairly general conditions, the matrix elements of the exciton-phonon interaction can easily be calculated if we go from the coordinates  $\mathbf{r}_e$  and  $\mathbf{r}_h$  to the coordinates  $\mathbf{x}$  and  $\mathbf{X}$ :

$$V_{nlm} \begin{pmatrix} \nu_2 \\ \nu_1 \end{pmatrix} = -\frac{ef_{nl}}{\sqrt{4\pi}} \delta_{m, m_2 - m_1 + n'_2 - m'_1} \sum_{p, s=0}^{\infty} i^{p+s-l} \times \frac{(2p+1)(2s+1)}{\sqrt{2l+1}} \sqrt{\frac{(2l_1+1)(2l'_1+1)}{(2l_2+1)(2l'_2+1)}} \times I_{n'_2, l'_2; n'_1, l'_1}^{n, l; p} J_{n_2, l_2; n_1, l_1}^{n, l; s} C_{l'_1, 0; p, 0}^{l'_2, 0} \times C_{l'_1, m'_1; p, m'_2 - m'_1}^{l'_2, m'_2} C_{s, 0; p, 0}^{l, 0} C_{s, m_2 - m_1; p, m'_2 - m'_1}^{l, m} \times C_{l_1, 0; s, 0}^{l_2, 0} C_{l_1, m_1; s, m_2 - m_1}^{l_2, m_2}. \quad (8)$$

Here  $C_{l_1, m_1; l_2, m_2}^{l, m}$  are Clebsch-Gordan coefficients<sup>19</sup> with the phases defined in accordance with Ref. 20. Combinations of Clebsch-Gordan coefficients completely determine the selection rules for exciton-exciton transitions involving  $LO$ -phonons in a quantum dot. The quantities symmetric in pairs of lower indices,

$$I_{n'_2, l'_2; n'_1, l'_1}^{n, l; p} = \frac{2}{j_{l'_2+1}(\xi_{n'_2, l'_2}) j_{l'_1+1}(\xi_{n'_1, l'_1})} \times \int_0^1 dy y^2 j_{l'_2}(y \xi_{n'_2, l'_2}) j_{l'_1}(y \xi_{n'_1, l'_1}) j_p(y \xi_{nl}) \quad (9)$$

are independent of  $R$  and are related to the radial part of the exciton wave functions of translational motion, which according to Refs. 1, 2, and 4 is proportional to  $j_{l'_i}(\xi_{n'_i, l'_i} X/R)$ . The quantities

$$J_{n_2, l_2; n_1, l_1}^{n, l; s} = \int_0^{\eta R} dx x^2 \left( j_s \left( \rho_h \xi_{nl} \frac{x}{R} \right) - (-1)^s j_s \left( \rho_e \xi_{nl} \frac{x}{R} \right) \right) F_{n_2, l_2}(x) F_{n_1, l_1}(x), \quad (10)$$

with

$$1 \leq \eta \leq 2, \quad (11)$$

are determined by the radial part  $F_{n_i, l_i}(x)$  of the wave functions of electron-hole relative motion. Equation (10) shows that the  $J_{n_2, l_2; n_1, l_1}^{n, l; s}$  are nonzero for even values of  $s$  only due to the difference between  $m_e$  and  $m_h$ . But according to the properties of the Clebsch-Gordan coefficient  $C_{l_1, 0; s, 0}^{l_2, 0}$  in (8), even values of  $s$  correspond to transitions between excitonic states whose angular momenta related to the relative motion of the electron and hole have the same parity, i.e.,  $l_1 + l_2 = 2t$ , where  $t$  is a nonnegative integer. This implies, in particular, that the diagonal part of the exciton-phonon interaction is nonzero only when  $m_e \neq m_h$ , i.e., when the extent to which the electron in the exciton is localized in space differs from the extent to which the hole is localized.

The uncertainty in the upper limit of integration in (10) characterized by the parameter  $\eta$  of (11) has profound physical meaning. The problem is that the problem of an electron and a hole coupled by the Coulomb potential and moving in the quantum well

$$U(\mathbf{r}_e, \mathbf{r}_h) = U(\mathbf{r}_e) + U(\mathbf{r}_h), \quad (12)$$

$$U(\mathbf{r}) = \begin{cases} 0, & |\mathbf{r}| \leq R, \\ \infty, & |\mathbf{r}| > R, \end{cases} \quad (13)$$

cannot be solved exactly, since it is actually a three-body problem<sup>21</sup> in which the well acts as the third particle. When expressed in terms of coordinates  $\mathbf{x}$  and  $\mathbf{X}$ , the quantum-well potential has an extremely complicated form  $U(\mathbf{X} + \mathbf{x}\rho_h, \mathbf{X} - \mathbf{x}\rho_e)$ , which cannot be expressed solely in terms of  $R$  and does not allow for separation of variables.

Thus, the eigenfunctions of the problem of an exciton in a quantum dot cannot generally be represented by the product (5). One way to avoid this difficulty in the weak confinement regime is to use a "pseudopotential" instead of  $U(\mathbf{X} + \mathbf{x}\rho_h, \mathbf{X} - \mathbf{x}\rho_e)$ , and choose it according to considerations of physical reason and maximum simplicity. This leads to uncertainty in the upper limit of integration in (10).

Indeed, while the inequality  $|\mathbf{X}| \leq R$  can serve as the natural (but somewhat overly restrictive) boundary condition on the position of the center of mass, for the distance between the electron and hole we can specify only the region where the boundary is located,  $R \leq |\mathbf{x}| \leq 2R$ . The lower limit in this double inequality corresponds to the case in which one of the particles comprising the exciton is at the center of the quantum dot, while the upper limit is attained when the electron and hole are located at opposite ends of the diameter of the quantum dot.

The pseudopotential  $U(\mathbf{X})$  (see Ref. 1) is still used in describing the excitonic regime. It allows for confinement only in translational exciton motion, and its sole (but extremely important) advantage is its exceptional simplicity.

The problem of an exciton moving in the pseudopotential  $U(\mathbf{X})$  can be solved exactly, and its eigenfunction are given by (5). Here the wave functions  $\Psi_{n'l'm'_i}(\mathbf{X})$  correspond to the size quantization levels that emerge as a result of the splitting of excitonic bands,<sup>1,2,4</sup> and the wave functions  $\psi_{n,l,m_i}(\mathbf{x})$  are the hydrogenlike wave functions of the Wannier exciton.<sup>22</sup> This approach is physically meaningful if

$$\psi_{n,l,m_i}(\mathbf{x}) \propto \exp\left(-\frac{x}{n_i R_{ex}}\right) \quad (14)$$

and if the region of localization of these wave functions,  $n_i R_{ex}$  is much smaller than  $\eta R$ .

All this significantly limits the applicability of the approach, particularly in describing multi-quantum processes, where one must allow for a large number of intermediate states.

The energy spectrum of an exciton in the pseudopotential  $U(\mathbf{X})$  can be written as follows:

$$E_{n'l'i}^{n'l'i} = E_g + \text{Ry} \left( -\frac{1}{n_i^2} + \frac{\mu}{M} \left( \frac{\xi_{n'l'i}}{d} \right)^2 \right), \quad (15)$$

where  $d = R/R_{ex}$ ,  $\mu = m_e m_h / M$ ,  $\text{Ry} = \mu e^4 / 2\epsilon_0^2 \hbar^2$  is the exciton rydberg, and  $E_g$  is the band gap of the bulk semiconductor. Bearing in mind that  $d = R/R_{ex} \gg 1$  and that the wave functions of relative motion have the form (14), we can replace the upper limit of the integral in (10) with  $\infty$ . The

result is a set of simple relationships for the matrix elements of the exciton-phonon interaction, which can be used for doing order-of-magnitude estimates and illustrating the qualitative aspects of this interaction.

Before we begin to analyze the matrix elements (8) of the exciton-phonon interaction, let us briefly examine the quantum-dot pseudopotential

$$U(\mathbf{X}) + U(\eta \mathbf{x}), \quad (16)$$

which, we believe, provides a better description of the exciton energy spectrum in the weak confinement regime, since the second term in (16) allows for the effect of the spatial constraint on relative electron-hole motion.

The eigenvalue problem for an exciton in the pseudopotential (16) can be solved exactly. As before, the wave functions have the form (5), with the  $\Psi_{n'l'm'_i}(\mathbf{X})$  coinciding with the wave functions for translational motion in the pseudopotential  $U(\mathbf{X})$ , while the radial part  $\psi_{n,l,m_i}(\mathbf{x})$  is now given by

$$F_{nl}(x) = A_{nl} \left( c_{nl} \frac{x}{R} \right)^l \exp\left(-\frac{c_{nl} x}{2R}\right) \times M\left(a_{nl} + l + 1, 2l + 2, c_{nl} \frac{x}{R}\right), \quad (17)$$

where  $M(a_{nl} + l + 1, 2l + 2, c_{nl} x/R)$  is the Kummer function that is regular at zero,  $A_{nl}$  is a normalization constant, and for the sake of simplicity the subscript  $i$  on the quantum numbers  $n$  and  $l$  of relative motion is dropped.

The boundary condition  $F_{nl}(\eta R) = 0$  is actually an eigenvalue equation. Negative and positive eigenvalues must be considered separately. In the first case, the energy of electron-hole relative motion is

$$E_{nl} = \text{Ry} \sum_{nl}(d) = -\frac{\text{Ry}}{N_{nl}^2(d)}, \quad (18)$$

with  $a_{nl} = -N_{nl}(d)$  and  $c_{nl} = 2d/N_{nl}(d)$ , and  $N_{nl}(d)$  being the  $n$ th root of the equation

$$M\left(-N_{nl}(d) + l + 1, 2l + 2, \frac{2d\eta}{N_{nl}(d)}\right) = 0. \quad (19)$$

In the second case,

$$E_{nl} = \text{Ry} \sum_{nl}(d) = \text{Ry} k_{nl}^2(d), \quad (20)$$

where  $k_{nl}(d)$  is the corresponding root of the equation

$$\text{Re} \left\{ \exp(-id\eta k_{nl}(d)) M\left(\frac{i}{k_{nl}(d)} + l + 1, 2l + 2, i2d\eta k_{nl}(d)\right) \right\} = 0, \quad (21)$$

i.e.,  $a_{nl} = i/k_{nl}(d)$  and  $c_{nl} = i2d k_{nl}(d)$ . Thus, the total energy of an exciton in the pseudopotential (16) can be written as

$$E_{n'l'i}^{n'l'i} = E_g + \text{Ry} \left( \sum_{n'l'i}(d) + \frac{\mu}{M} \left( \frac{\xi_{n'l'i}}{d} \right)^2 \right). \quad (22)$$

We have thus obtained the entire energy spectrum for both positive and negative values of  $\Sigma_{n_i l_i}(d)$ . Let us list its main features related to the effect of confinement on relative electron-hole motion.

First, for any fixed value of  $d$ , the number of levels with a negative  $\Sigma_{n_i l_i}(d)$  is finite, progressively decreasing as  $d$  decreases, and there exists a critical value  $d_c$  at which levels of this type completely disappear. The pattern of disappearance is such that as  $d$  decreases, negative energies tend to zero and then change sign, i.e., the levels are pushed out of the Coulomb potential well, with the process initiated by confinement. Second, confinement lifts the degeneracy in the orbital quantum momentum  $l_i$  of relative motion, a process inherent in the pure Coulomb problem (15).

A more detailed discussion of the exciton motion in the pseudopotential (16) is beyond the scope of the present paper. We note, however, that the features of such motion listed above agree with the results of Ref. 3 obtained by direct numerical calculation of the energy spectrum of the electron-hole pair in the initial potential (12) of a quantum dot.

We now discuss in more detail the matrix elements (8) of the exciton-phonon interaction for several low-energy excitonic states, which under optical excitation exhibit the features induced by confinement in the experimental spectra of systems with quantum dots most vividly. To analyze these matrix elements we use the exciton wave functions related to the pseudopotential  $U(\mathbf{X})$ . Of special interest are the excitonic states with  $l'_i = l_i = 0$ , whose excitation is possible in one-photon dipole-allowed transitions.

If we introduce the notation  $\nu_a(n'_i, n_i) = \{n'_i, 0, 0; n_i, 0, 0\}$ , from (8) we easily find that

$$V_{nlm} \begin{pmatrix} \nu_a(n'_2, n_2) \\ \nu_a(n'_1, n_1) \end{pmatrix} = -\frac{ef_{n0}}{\sqrt{4\pi}} \delta_{l,0} \delta_{m,0} J_{n'_2,0;n'_1,0}^{n,0;0} J_{n_2,0;n_1,0}^{n,0;0}, \quad (23)$$

where

$$J_{n'_2,0;n'_1,0}^{n,0;0} = \frac{1}{2n\pi} (\text{Si}[\pi(n-n'_1+n'_2)] + \text{Si}[\pi(-n+n'_1+n'_2)] - \text{Si}[\pi(-n-n'_1+n'_2)] - \text{Si}[\pi(n+n'_1+n'_2)]), \quad (24)$$

with  $\text{Si}(x)$  the sine integral, and the coefficients  $J_{n'_2,0;n'_1,0}^{n,0;0}$  for  $n_i = 1, 2$  have the form

$$J_{1,0;1,0}^{n,0;0} = \frac{1}{(1+\alpha_{nl}^h/4)^2} - \frac{1}{(1+\alpha_{nl}^e/4)^2}, \quad \alpha_{nl}^{h(e)} = \left( \frac{\xi_{nl} \rho_{h(e)}}{d} \right)^2, \quad (25)$$

$$J_{2,0;1,0}^{n,0;0} = J_{1,0;2,0}^{n,0;0} = 4\sqrt{2} \left( \frac{2}{3} \right)^6 \left( \frac{\alpha_{nl}^h}{(1+4\alpha_{nl}^h/9)^3} - \frac{\alpha_{nl}^e}{(1+4\alpha_{nl}^e/9)^3} \right), \quad (26)$$

$$J_{2,0;2,0}^{n,0;0} = \frac{(1-\alpha_{nl}^h)(1-2\alpha_{nl}^h)}{(1+\alpha_{nl}^h)^4} - \frac{(1-\alpha_{nl}^e)(1-2\alpha_{nl}^e)}{(1+\alpha_{nl}^e)^4}. \quad (27)$$

Equation (23) implies that the matrix elements between states of type  $\nu_a(n'_i, n_i)$  are nonzero only if completely sym-

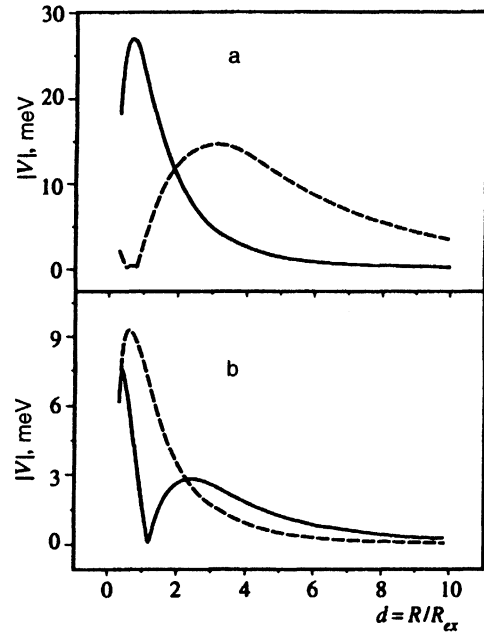


FIG. 1. The matrix elements for the interaction of an exciton with completely symmetric phonons of the  $\{100\}$  mode as functions of the relative quantum-dot radius: (a) (the diagonal part of the interaction) the solid curve corresponds to  $V_{100}(\nu_a^{(1,1)})$ , and the dashed curve to  $V_{100}(\nu_a^{(1,2)})$ ; and (b) (the off-diagonal part of the interaction) the solid curve corresponds to  $V_{100}(\nu_a^{(1,2)})$ , and the dashed curve to  $V_{100}(\nu_a^{(2,1)})$ . The parameters of the material are those of CuBr.

metric phonons (i.e., with  $l=m=0$ ) participate in the transition. Equations (25)–(27) show that these matrix elements are proportional to the effective mass difference,  $m_e - m_h$ , i.e., the part of the exciton-phonon interaction defined by (23) is related to the difference in the extent of spatial localization of the electron and hole in the exciton.

Since the magnitude of the exciton-phonon interaction strongly depends on the specific parameters of the quantum dot material, all further estimates and illustrative diagrams deal with CuBr:  $m_e = 0.28m_0$ ,  $m_h = 1.4m_0$  (the effective mass of heavy holes),  $R_{ex} = 1.25$  nm,  $\epsilon_0 = 8.6$ ,  $\epsilon_\infty = 4.6$ , and  $\omega^{LO} = 21.5$  meV. The reason why we chose this semiconductor is that secondary multiphonon emission in the two-photon resonant stationary excitation in the  $Z_{1,2}$  band of an exciton was first discovered in a system of quantum dots with an average radius  $R_0 = 3.2$  nm manufactured from this material.<sup>15</sup>

Figure 1a depicts the size dependence of the absolute value of the diagonal matrix elements  $V_{100}(\nu_a^{(1,1)})$  and  $V_{100}(\nu_a^{(1,2)})$ , which determine the scattering by a completely symmetric phonon  $\{100\}$ . These quantities and similar ones (for phonons  $\{n,0,0\}$  with  $n > 1$ ) comprise the Huang-Rees factor,<sup>23</sup> which plays an important role in multiphonon absorption, luminescence, and resonant Raman and hyper-Raman scattering of light. A similar dependence for the off-diagonal matrix elements  $V_{100}(\nu_a^{(1,2)})$  and  $V_{100}(\nu_a^{(2,1)})$  is depicted in Fig. 1b. Such quantities determine the lifetime of

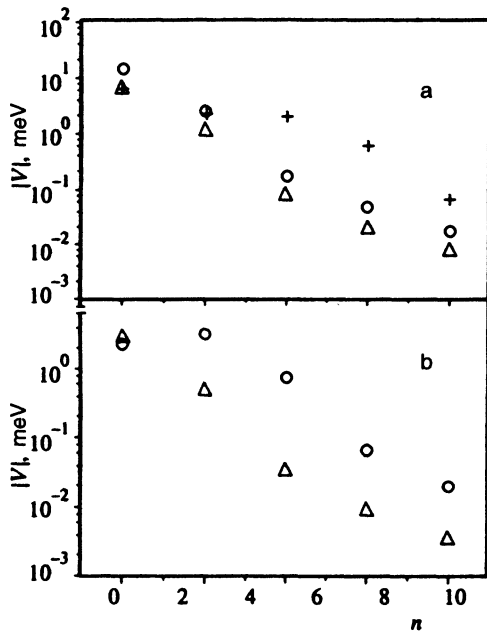


FIG. 2. The matrix elements of the interaction of an exciton with completely symmetric phonons as functions of the phonon quantum number  $n$  for a quantum dot of radius  $R = 2.56R_{ex}$ : (a) (the diagonal part of the interaction)  $\Delta$  corresponds to  $V_{n00}(\nu_a(1,1))$ ,  $\circ$  to  $V_{n00}(\nu_a(1,2))$ , and  $+$  to  $V_{n00}(\nu_a(2,1))$ ; and (b) (the off-diagonal part of the interaction)  $\Delta$  corresponds to  $V_{n00}(\nu_a(1,2))$ , and  $\circ$  to  $V_{n00}(\nu_a(2,1))$ . The parameters of the material are those of CuBr.

excitonic levels and contribute to resonant Raman and hyper-Raman scattering of light.

Figure 1 shows that the size dependence of the exciton-phonon interaction possesses a structure determined by the factor  $J_{n_2,0;n_1,0}^{n,0;0}$ , which is related to the hydrogenlike wave functions. However, there is no real sense in discussing this structure because it is situated in the range of quantum-dot sizes where the spatial constraint on the relative electron-hole motion must be taken into account. Theoretically, this can be done if in calculating the matrix elements we use the system of wave functions (17). A fact that can be considered firmly established is that as the quantum-dot size decreases and reaches the intermediate confinement region, the amplitudes of the transition matrix elements between excitonic states of type  $\nu_\alpha(n'_i, n_i)$  increase. Moreover, as  $R \rightarrow \infty$ , which means passing to the case of a bulk semiconductor, the matrix elements under discussion vanish like  $R^{-5/2}$ , as expected.

Figure 2 illustrates the magnitude of the interaction of an exciton with completely symmetric phonons as a function of the phonon quantum number  $n$ . We see that as  $n$  grows, the amplitude of the corresponding matrix elements sharply decreases, since its asymptotic behavior has the form of  $n^{-8}$ .

Using these results, we can answer the long-debated question about the size dependence of the Huang-Rees factor (see, e.g., Ref. 9). Let us estimate the Huang-Rees factor

$$S_{\nu_i} = \sum_{nlm} \frac{1}{(\hbar \omega_{nl}^{LO})^2} \left| V_{nlm} \begin{pmatrix} \nu_i \\ \nu_i \end{pmatrix} \right|^2, \quad (28)$$

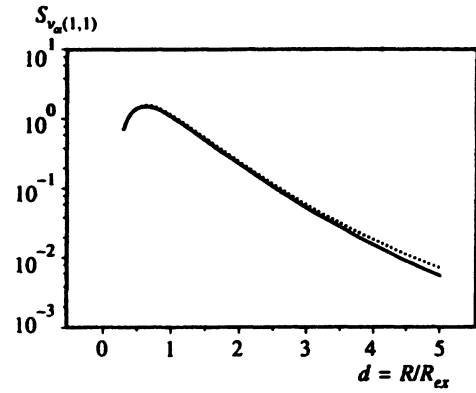


FIG. 3. The upper and lower bounds on the Huang-Rees factor as functions of the quantum-dot radius. The parameters of the material are those of CuBr: the solid curve corresponds to  $S^{\min}$ , and the dashed curve to  $S^{\max}$ .

restricting our discussion, for the sake of definiteness, to the ground state  $\nu_a(1,1)$  of an exciton in a quantum dot. To calculate

$$S_{\nu_a(1,1)} = \sum_{n=1}^{N_0(R)} \frac{1}{(\hbar \omega_{n0}^{LO})^2} \left| V_{n00} \begin{pmatrix} \nu_a(1,1) \\ \nu_a(1,1) \end{pmatrix} \right|^2 \quad (29)$$

exactly, we must know the mode composition of the natural vibrations of the spherical nanocrystal as a function of  $R$ , i.e., find the frequencies  $\omega_{n0}^{LO}$  and the number  $N_0(R)$  of distinct completely symmetric modes.

Such a calculation constitutes a problem in its own right. Hence we estimate the upper ( $S^{\max}$ ) and lower ( $S^{\min}$ ) bounds on (29), replacing  $\omega_{n0}^{LO}$  by an average frequency  $\omega^{LO}$  determined, say, from experiments in resonant Raman scattering of light. The bound  $S^{\min}$ , obviously, corresponds to the case in which there is only one completely symmetric vibration with  $n=1$ :

$$S^{\min} = \frac{1}{(\hbar \omega^{LO})^2} \left| V_{100} \begin{pmatrix} \nu_a(1,1) \\ \nu_a(1,1) \end{pmatrix} \right|^2, \quad (30)$$

and  $S^{\max}$  can be obtained if we assume that all  $LO$  vibrations of the quantum dot are completely symmetric.

As is known, the number  $N^{LO}$  of  $LO$ -modes in a diatomic crystal is equal to the number of unit cells in the crystal's volume. This immediately suggests that for a quantum dot  $N^{LO}(R) = 4\pi R^3/3V_c$ , where  $V_c$  is the unit cell volume. Then the upper bound on (29) can be obtained by putting  $N_0(R) = N^{LO}(R)$ .

Figure 3 depicts the upper and lower bounds on the Huang-Rees factor (29) as functions of the quantum-dot radius. The calculation was done for the parameters of CuBr:  $V_c = 0.183 \text{ nm}^3$ . We see that as  $R$  increases, so does the difference between  $S^{\max}$  and  $S^{\min}$ , but even for  $d=5.0$  this difference does not exceed 30%, although in calculating  $S^{\max}$  we allowed for 5580 terms in (29). Note that allowing for the first two terms in (29), i.e., taking into account only two completely symmetric modes, diminishes the difference between  $S_{\nu_a(1,1)}$  and  $S^{\max}$  at  $d=5.0$  to 0.3%.

Thus, we conclude that the Huang-Rees factor strongly depends on the size of the nanocrystal and, over the range of

sizes most interesting from the experimenter's viewpoint, can be approximated to high accuracy by several terms in (29). For order-of-magnitude estimates Eq. (30) is sufficient. Obviously, these features of the Huang–Rees factor are related to the aforementioned asymptotic behavior of the diagonal matrix element of the exciton–phonon interaction as functions of the quantum-dot radius  $R$  and the phonon quantum number  $n$ .

Note that according to Ref. 9, the Huang–Rees factor is independent of  $R$ . We believe, however, that this assumption is invalid and that the reason for such an erroneous conclusion lies in the fact that Klein *et al.*<sup>9</sup> chose a model exciton with an infinitely heavy hole and a fixed position of the center of mass, a model proposed by Merlin *et al.*<sup>24</sup> for describing multiphonon processes in bulk materials and unsuitable for quantum dots.

Another important class of matrix elements of the exciton–phonon interaction describes transitions between excitonic states of the type  $\nu_a(n'_i, n_i)$  and states that cannot be excited in one-photon dipole-allowed transitions. For the sake of definiteness, we take the matrix elements that link the ground excitonic state  $\nu_a(1,1)$  and states of type  $\nu_b(n'_i, l'_i, m'_i) = \{n'_i, l'_i, m'_i; 1, 0, 0\}$ :

$$V_{nlm} \left( \begin{array}{c} \nu_b(n' l' m') \\ \nu_a(1,1) \end{array} \right) = - \frac{ef_{nl}}{\sqrt{4\pi}} \delta_{l,l'} \delta_{m,m'} J_{n',l';1,0}^{n,l;l} J_{1,0;1,0}^{n,l;0}, \quad (31)$$

where we have dropped the subscript  $i$  for the sake of simplicity. We see that the phonons participating in the given transitions are those whose angular momentum  $l$  and its projection  $m$  coincide with the corresponding quantum numbers of the final excitonic states.

The matrix elements (31) are interesting because they describe two important effects associated with vibrational resonance of the initial and final excitonic states. Indeed, if the quantum dot has a radius  $R$  such that the energy gap between the levels  $\nu_b(n' l' m')$  and  $\nu_a(1,1)$  is close to the phonon energy  $\hbar\omega_{nl}^{LO}$ , or

$$R = R_{ex} \sqrt{\frac{Ry}{\hbar\omega_{nl}^{LO}} \frac{\mu}{M} (\xi_{n',l'}^2 - \pi^2)}, \quad (32)$$

the exciton–vibrational interaction is resonant, and even for a moderate value of the matrix element leads to renormalization of the vibrational frequency and formation of an exciton–phonon complex, as happens in bulk materials.<sup>25</sup>

The same resonance allows for the possibility of double optical–vibrational resonance occurring in one-photon transitions when the photon energy  $\hbar\omega$  is close to the energy necessary for producing an exciton in the ground state.

Figure 4a depicts the size dependence of the absolute value of the matrix elements

$$V_{n1m} \left( \begin{array}{c} \nu_b(11m') \\ \nu_a(1,1) \end{array} \right)$$

for  $n=1, 2$ , which describe transitions involving threefold degenerate phonons  $\{11m\}$  and  $\{21m\}$ . We see that over the important range of quantum-dot sizes,

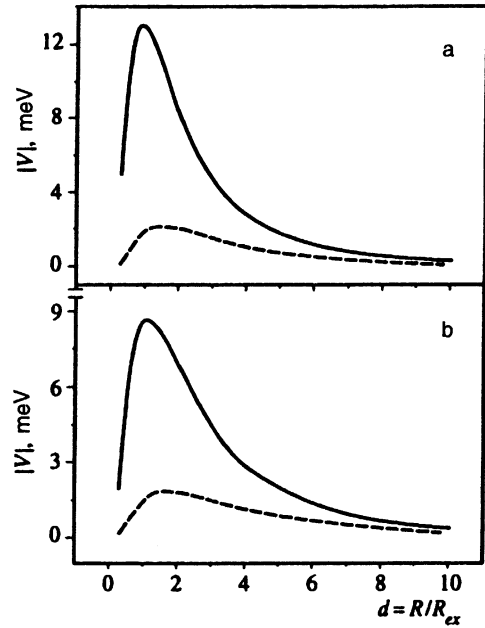


FIG. 4. (a) The size dependence of the exciton–phonon interaction matrix elements  $V_{n1m}(\nu_b(11m'), \nu_a(1,1))$ , which determine a possible vibrational resonance with a  $\{11m\}$  phonon mode (solid curve) and a  $\{21m\}$  phonon mode (dashed curve); (b) the size dependence of the reduced matrix elements of the Jahn–Teller interaction,  $V_{n2m}(\nu_b(11m'_i), \nu_a(1,1))/\hat{W}_m$ , with a phonon of mode  $\{12m\}$  (solid curve) and a phonon of mode  $\{22m\}$  (dashed curve). The parameters of the material are those of CuBr.

$$V_{n1m} \left( \begin{array}{c} \nu_b(11m') \\ \nu_a(1,1) \end{array} \right)$$

is comparable in order of magnitude to

$$V_{n10} \left( \begin{array}{c} \nu_a(1,1) \\ \nu_a(1,1) \end{array} \right)$$

and depends on the phonon quantum number  $n$  in a similar way. The latter is due to the fact that asymptotically the matrix elements considered here behave like  $n^{-7}$ .

In conclusion we examine the exciton–phonon interaction of the Fröhlich type (Eq. (8)) from the viewpoint of the Jahn–Teller effect. This effect occurs only if the excitonic state is degenerate. For the sake of simplicity we restrict our discussion to the threefold degenerate state  $\nu_b(11m'_i)$ . Other cases can be treated by reasoning along similar lines. Then, according to (8), the properties of the Clebsch–Gordan coefficients suggest that an exciton in the given state can interact with completely symmetric phonons  $\{n00\}$  and with fivefold degenerate phonons  $\{n2m\}$ . In the first case the matrix elements (8) are diagonal and proportional to the identity  $m' \times m'$  matrix formed from  $C_{1,0;0,0}^{1,0} C_{1,m'_i;0,0}^{1,m'_i}$ :

$$V_{n00} \left( \begin{array}{c} \nu_b(11m'_2) \\ \nu_b(11m'_1) \end{array} \right) = - \frac{ef_{n0}}{\sqrt{4\pi}} J_{1,1;1,1}^{n,0;0} J_{1,0;1,0}^{n,0;0} \begin{pmatrix} 1 & 0 & 0 \\ 0 & 1 & 0 \\ 0 & 0 & 1 \end{pmatrix}. \quad (33)$$

Thus, as expected, completely symmetric phonon modes are inactive in the Jahn–Teller effect. The situation is dramatically different for the interaction with  $\{n2m\}$  phonons,

$$V_{n2m} \begin{pmatrix} \nu_b(11m'_2) \\ \nu_b(11m'_1) \end{pmatrix} = \frac{efn_2}{\sqrt{4\pi}} J_{1,1;1,1}^{n,2;2} J_{1,0;1,0}^{n,2;0} \hat{W}_m, \quad (34)$$

where the matrices  $\hat{W}_m$  have the following form:

$$\begin{aligned} \hat{W}_2 &= \hat{W}_{-2}^+ = \sqrt{\frac{6}{5}} \begin{pmatrix} 0 & 0 & 1 \\ 0 & 0 & 0 \\ 0 & 0 & 0 \end{pmatrix}, \\ \hat{W}_1 &= -\hat{W}_{-1}^+ = \sqrt{\frac{3}{5}} \begin{pmatrix} 0 & -1 & 0 \\ 0 & 0 & 1 \\ 0 & 0 & 0 \end{pmatrix}, \\ \hat{W}_0 &= \sqrt{\frac{1}{5}} \begin{pmatrix} 1 & 0 & 0 \\ 0 & -2 & 0 \\ 0 & 0 & 1 \end{pmatrix}. \end{aligned} \quad (35)$$

The rows  $m'_2$  and columns  $m'_1$  in (35) are numbered 1, 0, and  $-1$ .

From (34) and (35) we see that the  $\{n2m\}$  phonons are active in the Jahn–Teller effect and that the emerging problem can be reduced to the so-called  $T \otimes d$ -problem, known from the theory of vibronic interactions in molecular and impurity systems.<sup>26</sup> Without going into details, we merely note that as a result of the dynamic Jahn–Teller effect there emerges an exciton–phonon complex with a many-sheeted and multimimum vibrational adiabatic potential, and that the initial threefold degenerate excitonic state splits.

Figure 4b depicts the size dependence of the absolute values of the exciton–phonon interaction matrix elements (34) (the factors of the matrices  $\hat{W}_m$ ) describing the interaction with  $\{12m\}$  and  $\{22m\}$  phonons. We see that the amplitude of these Jahn–Teller matrix elements and the amplitudes of (23) and (31) are of the same order of magnitude at equal values of the phonon quantum number  $n$  (see Figs. 1a and 4a).

At first glance it might seem that it is difficult to spot in experiments the Jahn–Teller effect considered here, since one-photon transitions into the excitonic states  $\nu_b(11m'_i)$  are forbidden in the dipole approximation. However, these states are accessible in two-photon excitation, and furthermore, when the excitonic ground state is in the aforementioned resonance with  $\nu_b(11m'_i)$ , the Jahn–Teller effect is also exhibited by the one-photon spectra of quantum dots.

### 3. MULTIPHONON ABSORPTION OF LIGHT IN QUANTUM DOTS

We illustrate the above results with multiphonon light absorption involving one-photon excitation of the excitons. As noted earlier, in the weak confinement regime the diagonal part of the exciton– $LO$ -phonon interaction is nonzero. Its contribution to multiphonon absorption or luminescence can be estimated by employing the form functions of the corresponding spectra.

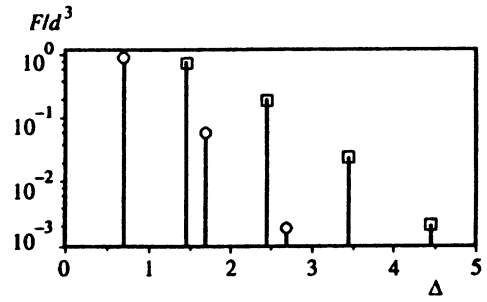


FIG. 5. The dependence of the form functions of multiphonon light absorption on the frequency detuning for two quantum-dot sizes (CuBr). The luminescence spectrum can be obtained via mirror reflection of the corresponding picket fence about the phononless line (the line with the lowest frequency):  $\square$  corresponds to  $d=2.0$ , and  $\circ$  to  $d=3.0$ .

In our model and in the dipole approximation, only excitonic states with  $l'_1=l_1=0$  can be excited in one-photon transitions. When an exciton interacts with a single vibrational mode, the form function of the absorption spectrum has the form

$$\begin{aligned} F(\Delta) &= d^3 \sum_{n'_1 n_1} \frac{1}{(n'_1)^2 (n_1)^3} \exp(-S_{\nu_a(n'_1, n_1)} \coth \beta) \\ &\times \sum_{t=-\infty}^{\infty} \exp(t\beta) I_t \left( \frac{2S_{\nu_a(n'_1, n_1)}}{\sinh \beta} \right) \\ &\times \delta \left( \Delta - \frac{E_{n'_1 0}^{n_1 0} - E_g + Ry}{\hbar \omega^{LO}} + S_{\nu_a(n'_1, n_1)} - t \right), \end{aligned} \quad (36)$$

where

$$\Delta = \frac{\hbar \omega - E_g + Ry}{\hbar \omega^{LO}}, \quad (37)$$

$\omega$  is the frequency of the light,  $\beta = \hbar \omega^{LO}/2T$ ,  $T$  is the temperature in energy units,  $I_t(x)$  is the modified Bessel function, and  $E_{n'_1 0}^{n_1 0}$  is defined in (15).

The fact that the single-mode approximation can be used follows from the dependence of the diagonal matrix elements of the interaction on the phonon quantum number  $n$  discussed earlier. Thus, we can assume that  $\omega^{LO} = \omega_{10}^{LO}$ .

A similar expression can easily be written for the form function of the equilibrium luminescence spectrum. Equation (36) shows that owing to the presence of the factor  $(n'_1)^{-2} (n_1)^{-3}$  the main contribution to  $F(\Delta)$  is provided by the first excitonic level with  $n'_1=n_1=1$ . Below we restrict our discussion to this part of the absorption form function. We also assume that there is no vibrational resonance between the ground and excited exciton states.

The dependence of the absorption form function at liquid helium temperatures and CuBr parameters on the frequency detuning  $\Delta$  is depicted in Fig. 5. As expected,  $F(\Delta)$  is a picket fence with a period equal to the optical phonon energy. In real situations, however, there are reasons why the lines in the picket fence broaden. One of the most important reasons for homogeneous broadening is related to the finite

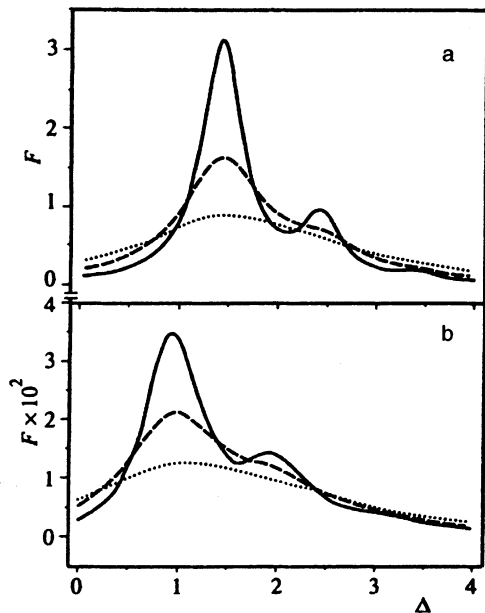


FIG. 6. The form-function spectra of multiphonon light absorption with allowance for the finite width  $\gamma$  of the excitonic level: (a) for a quantum dot of radius  $R=2.0R_{ex}$ , and (b) for an ensemble of quantum dots with the Lifshits-Slezov size distribution function (the average radius  $R_0=2.0R_{ex}$ ). The parameters of the material are those of CuBr, the solid curves correspond to  $\gamma=0.5\omega^{LO}$ , the dashed curves to  $\gamma=1.0\omega^{LO}$ , and the dotted curves to  $\gamma=2.0\omega^{LO}$ .

lifetime of exciton-vibrational states, which can easily be taken into account in (36) by replacing the delta function  $\delta(x)$  with its representation in terms of a Lorentzian with a phenomenological width  $\gamma/\omega^{LO}$ :

$$\frac{\gamma}{2\pi\omega^{LO}} \frac{1}{x^2 + (\gamma/2\omega^{LO})^2}. \quad (38)$$

Figure 6a depicts the  $\Delta$ -dependence of a homogeneously broadened absorption form function for three values of the parameter  $\gamma/\omega^{LO}$ . At moderate values of  $\gamma$  the phononless line and its one-phonon replica are clearly visible.

Note that Eq. (36) describes absorption by a system of equivalent quantum dots under identical conditions, which means that inhomogeneous broadening is not taken into account. However, the objects used in real experiments are characterized by absorption spectra with large inhomogeneous broadening related to variance in the quantum-dot sizes. The size distribution function of nanocrystals is determined by the way in which the specimen is manufactured; here the most readily available systems are those in which the quantum-dot radii are distributed according to the Lifshits-Slezov function<sup>27</sup> characterized by a single parameter  $R_0$ , the average radius. Figure 6b depicts the  $\Delta$ -dependence of the absorption form function in which both homogeneous and inhomogeneous broadening are taken into account. Clearly, the large asymmetry of the Lifshits-Slezov function leads to a long-wave shift in the absorption spectrum.

#### 4. CONCLUSION

In calculating the matrix elements of the exciton-phonon interaction we assumed that the potential of a quantum dot has infinitely high walls, and ignored the relationship between excitons and surface vibrational modes. But even without these restrictions the structure of (8) is the same. As before, the matrix elements are linear combinations of products of six Clebsch-Gordan coefficients determining the selection rules in spherically shaped nanocrystals.

At the same time, the analytic expressions for the weight factors, which specify the magnitude of the exciton-phonon interaction, differ considerably from (9) and (10). Therefore, it would be interesting to generalize the results of the present paper to these cases. In particular, allowing for surface modes could prove to be important in problems of vibrational and double optical-vibrational resonance and in the Jahn-Teller effect.

Another promising area in studies of the exciton-phonon interaction is the use of the pseudopotential (16), which takes confinement into account in the relative electron-hole motion. The system of the exciton wave functions in such a potential makes it possible to study the non-trivial size dependence of the exciton-phonon interaction mentioned in Sec. 2 in greater detail (Fig. 1). Preliminary estimates have revealed that the effect of confinement on the relative motion enhances the role that excited excitonic states play in the formation of the optical spectra of quantum dots. For instance, the contributions of the excitonic states with the principal quantum number  $n_1$  of relative motion to the multiphonon absorption form function (36) are no longer proportional to  $(n_1)^{-3}$ .

Below we list the results of our work.

a) We have derived analytic expressions for the exciton-vibrational interaction of the Fröhlich type in quantum dots in the weak confinement regime, and have established the selection rules for transitions between any excitonic levels. It has been found that because of three-dimensional confinement, the exciton-phonon interaction in transitions between states with the same parity (related to the relative electron-hole motion) loses its forbidden nature.

b) We have studied the size dependence of the exciton-phonon interaction matrix elements that describe the transitions between the lowest exciton levels. It has been established that the amplitude of the matrix elements sharply decreases with increasing phonon quantum number  $n$ . This makes it possible to use only a small number of vibrational modes, for example, in studying the cross sections and excitation profiles of resonant Raman and hyper-Raman scattering and in interpreting the corresponding experimental data.

c) We have estimated the Huang-Rees factor, which plays an important role in various multiphonon processes. It has been established that this factor strongly depends on the quantum-dot radius. On the basis of these results we have calculated the form function of the multiphonon absorption of light by a system of quantum dots with allowance for both homogeneous and inhomogeneous broadening.

d) We have shown that essentially quantum dots constitute a Jahn-Teller system. Moreover, under certain conditions, vibrational resonance between excitonic states can oc-

cur in a quantum dot. Both of these circumstances are known to lead to the formation of exciton–phonon complexes, which can be observed experimentally by employing the methods used in two-photon spectroscopy or optical–vibrational resonance spectroscopy.

e) We have proposed a new method for calculating the energy spectrum of an exciton in a quantum dot. It allows for the effect of confinement on the relative electron–hole motion and provides a complete set of excitonic states, which is extremely important in describing multiexciton processes.

The authors would like to express their gratitude to the Russian Fund for Fundamental Research for financial support (Projects Nos. 96-02-16235-a and 96-02-16242-a).

<sup>1</sup>Al. L. Éfros and A. L. Éfros, *Fiz. Tekh. Poluprovodn.* **16**, 772 (1982).

<sup>2</sup>E. Hanamura, *Phys. Rev. B* **37**, 1273 (1988).

<sup>3</sup>Y. Kayanuma, *Phys. Rev. B* **38**, 9797 (1988).

<sup>4</sup>S. Schmitt-Rink, D. A. Miller, and D. S. Chemla, *Phys. Rev. B* **35**, 8113 (1987).

<sup>5</sup>A. V. Fedorov, A. V. Baranov, and K. Inoue, submitted to *Phys. Rev. B* (1996).

<sup>6</sup>Yu. E. Perlin, *Usp. Fiz. Nauk* **80**, 553 (1963).

<sup>7</sup>Yu. E. Perlin and B. S. Tsukerblat, *Effects of Electron–Vibrational Interactions in the Optical Spectra of Paramagnetic Impurity Ions* [in Russian], Shtiintsa, Kishinev (1974).

<sup>8</sup>A. V. Fedorov, V. A. Kremerman, and A. I. Ryskin, *Phys. Rep.* **248**, 371 (1994); A. V. Fedorov, *Zh. Éksp. Teor. Fiz.* **105**, 1667 (1994) [*JETP* **78**, 899 (1994)].

<sup>9</sup>M. C. Klein, F. Hache, D. Ricard, and C. Flyzannis, *Phys. Rev. B* **42**, 11123 (1990).

<sup>10</sup>E. Roca, C. Trallero-Giner, and M. Cardona, *Phys. Rev. B* **49**, 13704 (1990).

<sup>11</sup>J. C. Marini, B. Stebe, and E. Kartheuser, *Phys. Rev. B* **50**, 14302 (1994).

<sup>12</sup>A. V. Baranov, Ya. S. Bobovich, and V. I. Petrov, *J. Raman Spectr.* **24**, 767 (1993).

<sup>13</sup>A. V. Baranov, K. Inoue, K. Toba, A. Yamanaka, V. I. Petrov, and A. V. Fedorov, *Phys. Rev. B* **53**, R1721 (1996).

<sup>14</sup>Y. Toyozawa and J. Hermanson, *Phys. Rev. Lett.* **21**, 1637 (1968).

<sup>15</sup>K. Inoue, A. V. Baranov, and A. Yamanaka, *Physica B* **6363** (1996).

<sup>16</sup>A. D. Yoffe, *Adv. Phys.* **42**, 173 (1993).

<sup>17</sup>A. I. Ansel'm and Yu. A. Firsov, *Zh. Éksp. Teor. Fiz.* **28**, 151 (1955); **30**, 719 (1956) [*Sov. Phys. JETP* **1**, 139 (1955); **3**, 564 (1956)].

<sup>18</sup>R. S. Knox, *Theory of Excitons*, Academic Press, New York (1963).

<sup>19</sup>D. A. Varshalovich, A. N. Moskalev, and V. K. Khersonskii, *Quantum Theory of Angular Momentum*, World Scientific, Singapore (1987).

<sup>20</sup>E. U. Condon and G. H. Shortley, *The Theory of Atomic Spectra*, Cambridge Univ. Press, London (1953).

<sup>21</sup>P. M. Morse and H. Feshbach, *Methods of Theoretical Physics*, McGraw-Hill, New York (1953).

<sup>22</sup>L. D. Landau and E. M. Lifshitz, *Quantum Mechanics: Nonrelativistic Theory*, 3rd ed., Pergamon Press, Oxford (1977).

<sup>23</sup>A. M. Stoneham, *Theory of Defects in Solids: Electronic Structure and Defects in Insulators and Semiconductors*, Oxford Univ. Press, Oxford (1975).

<sup>24</sup>R. Merlin, G. Güntherodt, M. Cardona, S. Suryanarayanan, and F. Holtzberg, *Phys. Rev. B* **17**, 4951 (1978).

<sup>25</sup>I. B. Levinson and É. I. Rashba, *Usp. Fiz. Nauk* **111**, 681 (1973); É. I. Rashba, *Zh. Éksp. Teor. Fiz.* **71**, 319 (1976) [*Sov. Phys. JETP* **44**, 166 (1976)].

<sup>26</sup>M. C. O'Brien, *J. Phys. C* **4**, 2524 (1971); I. B. Bersuker and V. Z. Polinger, *Vibronic Interactions in Molecules and Crystals*, Springer-Verlag, Berlin (1989).

<sup>27</sup>I. M. Lifshits and V. V. Slezov, *Zh. Éksp. Teor. Fiz.* **35**, 479 (1958) [*Sov. Phys. JETP* **8**, 331 (1959)].

Translated by Eugene Yankovsky